J|A|C|S COMMUNICATIONS

Published on Web 08/18/2010

Supercritical Fluid Synthesis of Magnetic Hexagonal Nanoplatelets of Magnetite

Zhonglai Li,[†,‡] Jeffrey F. Godsell,[§] Justin P. O'Byrne,[†,‡] Nikolay Petkov,[||] Michael A. Morris,[†,‡] Saibal Roy,[§] and Justin D. Holmes*[,†,‡]

Materials and Supercritical Fluids Group, Department of Chemistry, Microsystems Centre, and Electron Microscopy and Analysis Facility (EMAF), Tyndall National Institute, University College Cork, Lee Maltings, Prospect Row, Cork, Ireland, and Centre for Research on Adaptive Nanostructures and Nanodevices (CRANN), Trinity College Dublin, Dublin 2, Ireland

Received June 10, 2010; E-mail: j.holmes@ucc.ie

Abstract: A supercritical fluid technique was used to prepare hexagonal nanoplatelets of magnetite. Ferrocene was used as the Fe source, and sc-CO_2 acted as both a solvent and oxygen source in the process. Powder X-ray diffraction, transmission electron microscopy, X-ray photoelectron spectroscopy, and magnetic measurements were used to characterize the products. It was found that the morphology and structure of the product strongly depended on the reaction conditions.

The properties of nanomaterials have been shown to strongly depend on their morphology, microstructure, dimensions, and crystallinity.[1,2] Nanostructured iron oxides have been investigated by several research groups due to their potential applications in high-density recording media, ferrofluids, and magnetic sensors.[3] Various morphologies, including nanowires, size-monodispersed nanoparticles, and nanostructures encapsulated in carbon nanotubes,[4] have been prepared and investigated using different synthetic methods. For example, Suslick and co-workers successfully synthesized hollow nanosized hematite particles, using carbon nanoparticles as a template, by a sonochemical method.[5] Recently, ordered mesoporous iron oxide was prepared using an SBA-15 templated approach.[6] However, to the best of our knowledge, nanostructured cubic Fe_3O_4 with a hexagonal morphology has not been reported to date using any method.

Supercritical fluid (SCF) techniques have been utilized to synthesize various nanomaterials including Ge and Si nanowires and carbon nanotubes.[7] It is worth noting that supercritical carbon dioxide (sc-CO_2) is often used as a solvent for the formation of nanomaterials due to its negligible surface tension and low viscosity. In this communication we demonstrate for the first time that sc-CO_2 can be used as both a solvent and a reactant to form hexagonal nanoplatelets of Fe_3O_4. The synthesis is based on the thermal decomposition of ferrocene to reduced iron, followed by the subsequent oxidation of the iron particles by sc-CO_2. In a typical SCF experiment, a quartz boat containing 0.5 g of ferrocene was placed in the center of a high-pressure stainless steel reactor (Inconel 625 GR2- Snap-tite, Inc.).[8] The reactor was then charged with sc-CO_2 (T_c = 31 °C, P_c = 7.38 MPa) at 40 °C and 10.34 MPa and heated to a temperature between 650−750 °C in CO_2, with an outlet flow rate of 200 mL min^{-1} for 2 h.

The structure of the as-synthesized sample prepared at 750 °C and 10.34 MPa in sc-CO_2 was examined by powder X-ray diffraction (XRD) as shown in Figure 1. Six obvious diffraction peaks can be indexed as the (220), (311), (400), (422), (511), and (440) crystal faces of the cubic phase magnetite (Fe_3O_4; Joint Committee on Powder Diffraction Standards (JCPDS) File No. 11-0614). The intensities of the three main diffraction peaks correspond well with the JCPDS file, with the refined lattice parameter values of $a = b = c = 8.39$ Å.

In order to more accurately verify the phases, X-ray photoelectron spectroscopy (XPS) analysis of the iron oxide nanoplatelets was also undertaken (Figure S1, Supporting Information). The binding energies related to Fe $2p_{3/2}$ and Fe $2p_{1/2}$ are at approximately 711.3 and 724.5 eV, respectively, and the broad Fe 2p signals are attributed to the coexistence of Fe^{3+} and Fe^{2+} states.[9]

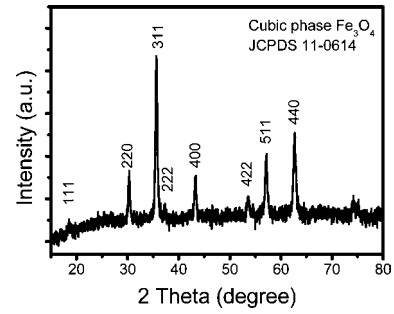

Figure 1. XRD pattern of the iron oxide product prepared at 750 °C and 10.34 MPa in sc-CO_2.

The morphology of the Fe_3O_4 product obtained is shown in Figure 2. A typical product prepared at 750 °C and 10.34 MPa exhibited well-defined hexagonal nanoplatelets with a mean diameter of 200 nm. The side-view image indicates that the thickness of the nanoplatelets was in the range of ca. 20−30 nm. The high-resolution transmission electron microscopy (HRTEM) image shows that the lattice spacing is about 0.49 nm, which can be assigned to the (111) plane of Fe_3O_4. It is noteworthy that the synthesized Fe_3O_4 metastable phase is unstable against further oxidation in air at 450 °C for 3 h, whereupon it is transformed to hematite (α-Fe_2O_3) (Figure S2, Supporting Information).[10] We also investigated the effect of the synthesis temperature on the morphology of the iron oxide nanomaterials but found that ball-like Fe_3O_4 platelets [(Figure S3, Supporting Information) were produced at temperatures approaching 650 °C instead of the desired hexagonal morphology. Hence, isotropic growth of iron oxide occurs at low temperatures in the SCF environment.

Figure 3 shows the magnetic properties of the hexagonal Fe_3O_4 platelets measured at room temperature. The platelets exhibited ferrimagnetic behavior, with saturation magnetization (M_s) = 51.4 emu/g, remanent magnetization (M_r) = 18.9 emu/g, and coercivity (H_c) = 263 Oe. The room-temperature ferrimagnetic behavior of

[†] Materials and Supercritical Fluids Group, Department of Chemistry, and Tyndall National Institute, University College Cork.
[‡] CRANN, Trinity College Dublin.
[§] Microsystems Centre, Tyndall National Institute, University College Cork.
[||] EMAF, Tyndall National Institute, University College Cork.

 10.1021/ja105079y

Fe_3O_4 platelets was expected, since the overall mean diameter of the particles (~200 nm) was above the single-domain size. Additionally, the saturation magnetization and remanent magnetization of Fe_3O_4 prepared at 750 °C are much larger than those of Fe_3O_4 prepared at 650 °C. The saturation magnetization and remanent magnetization of Fe_3O_4 prepared at 650 °C were 31.9 and 10.7 emu/g, respectively (Figure S4, Supporting Information).

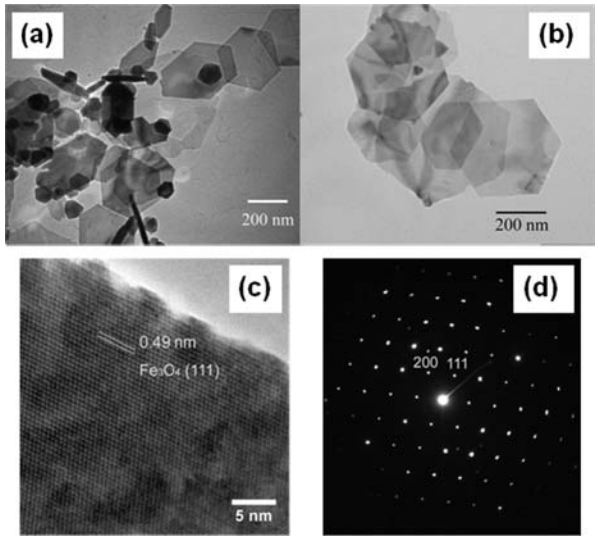

Figure 2. (a,b) TEM images, (c) HRTEM image, and (d) SAED pattern of the Fe_3O_4 product prepared at 750 °C and 10.34 MPa in sc-CO_2.

On the other hand, the saturation magnetization value of Fe_3O_4 is less than that for bulk magnetite (92 emu/g), as reported elsewhere.[11] The observed lower saturation magnetization value compared to that of the bulk may be attributed in part to an internal compensation within the spinel structure of the A and B magnetic sublattices.[12] The large surface-to-volume ratio of the nanoplatelets, compared to that of the bulk material, may also be a likely contributing factor to the reduced magnetization. Specifically, the width of the nanoplatelets, being 20−30 nm, is likely to cause spin frustration (spin-glass type) on their surface due to the random canting of surface spins. This phenomenon results in a disorder of the competing superexchange interactions between the Fe tetrahedral and octahedral sites within the unit cells, effectively weakening the overall exchange coupling in the Fe_3O_4 nanoplatelets.

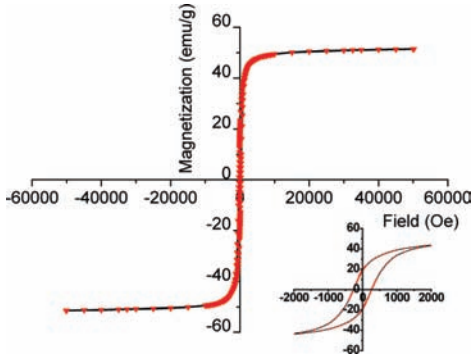

Figure 3. Magnetic hysteresis curve of Fe_3O_4 prepared at 750 °C and 10.34 MPa in sc-CO_2 (inset shows the hysteresis loop zoomed-in at the origin).

Ferrocene has previously been used as a precursor to synthesize carbon nanotubes and carbon-coated iron nanoparticles by chemical vapor and supercritical fluid deposition.[13] Fe particles formed by the thermal decomposition of ferrocene are able to catalytically generate carbons. In our experiments, undertaken in the presence of CO_2, it is assumed that the ferrocene first decomposes to form iron nanoparticles when heated above 600 °C.[14] The Fe nanoparticles formed react with sc-CO_2 to form the magnetite platelets, probably through aggregation, as Fe can reduce CO_2 to form iron oxide and CO.[15] In addition, any carbon byproducts formed can react with CO_2 to form CO.

In summary, we report the preparation of hexagonal magnetite nanoplatelets using a SCF method. CO_2 under supercritical fluid conditions is believed to serve as both a solvent and an oxygen source. sc-CO_2 and reaction temperature play important roles in the formation of magnetic hexagonal nanoplatelets of magnetite. The obtained magnetic nanomaterial may have potential applications in recording media and sensor devices.

Acknowledgment. The authors acknowledge financial support from Science Foundation Ireland (projects 07/SRC/I1172 and 06/IN.1/I98). This research was also enabled by the Higher Education Authority Program for Research in Third Level Institutions (2007−2011) via the INSPIRE programme. Z.L. thanks Dr. Fathima Laffir for XPS and Dr. Calum Dickinson for HRTEM measurements.

Supporting Information Available: XPS, TEM, XRD, and magnetic measurement results. This material is available free of charge via the Internet at http://pubs.acs.org.

References

(1) (a) Fernandez-Garcia, M.; Belver, C.; Hanson, J. C.; Wang, X.; Rodriguez, J. A. *J. Am. Chem. Soc.* **2007**, *129*, 13604–13612. (b) Mackenzie, J. D.; Bescher, E. P. *Acc. Chem. Res.* **2007**, *40*, 810–818. (c) Song, A. M.; Omling, P.; Samuelson, L.; Seifert, W.; Shorubalko, I.; Zirath, H. *Appl. Phys. Lett.* **2001**, *79*, 1357–1359. (d) Wang, X.; Zhuang, J.; Peng, Q.; Li, Y. *Nature* **2005**, *437*, 121–124. (e) Ahn, J.; Kim, H.; Lee, K.; Jeon, S.; Kang, S.; Sun, Y.; Nuzzo, R.; Rogers, J. *Science* **2006**, *314*, 1754–1757.

(2) (a) Tsuji, T.; Okazaki, Y.; Higuchi, T.; Tsuji, M. *J. Photochem. Photobiol. A: Chemistry* **2006**, *183*, 297–303. (b) Liu, X.; Qiu, G.; Wang, Z.; Li, X. *Nanotechnology* **2005**, *16*, 1400–1405. (c) Chen, W.; Pan, X.; Bao, X. *J. Am. Chem. Soc.* **2007**, *129*, 7421–7426.

(3) (a) Varanda, L.; Jafelicci, M.; Tartaj, P.; O'Grady, K.; Gonzalez-Carreno, T.; Morales, M.; Munoz, T.; Serna, C. *J. Appl. Phys.* **2002**, *92*, 2079–2085. (b) Vaishnava, P. P.; Tackett, R.; Dixit, A.; Sudakar, C.; Naik, R.; Lawes, G. *J. Appl. Phys.* **2007**, *102*, 063914−063918. (c) Jiang, J. Z.; Lin, R.; Lin, W.; Nielsen, K.; Mørup, S.; Dam-Johansen, K.; Clasen, R. *J. Phys. D* **1997**, *30*, 1459–1467.

(4) (a) Suber, L.; Imperatori, P.; Ausanio, G.; Fabbri, F.; Hofmeister, H. *J. Phys. Chem. B* **2005**, *109*, 7103–7109. (b) Wang, R.; Chen, Y.; Fu, Y.; Zhang, H.; Kisielowski, C. *J. Phys. Chem. B* **2005**, *109*, 12245–12249. (c) Cabot, A.; Puntes, V. F.; Shevchenko, E.; Yin, Y.; Balcells, L.; Marcus, M. A.; Hughes, S. M.; Alivisatos, A. P. *J. Am. Chem. Soc.* **2007**, *129*, 10358–10360. (d) Ye, E.; Liu, B.; Fan, W. Y. *Chem. Mater.* **2007**, *19*, 3845–3849.

(5) Bang, J. H.; Suslick, K. S. *J. Am. Chem. Soc.* **2007**, *129*, 2242–2243.

(6) Jiao, F.; Jumas, J.-C.; Womes, M.; Chadwick, A. V.; Harrison, A.; Bruce, P. G. *J. Am. Chem. Soc.* **2006**, *128*, 12905–12909.

(7) (a) Cooper, A. I. *Adv. Mater.* **2001**, *13*, 1111–1114. (b) Long, D. P.; Blackburn, J. M.; Watkins, J. J. *Adv. Mater.* **2000**, *12*, 913–915. (c) Lu, X.; Hanrath, T.; Johnston, K. P.; Korgel, B. A. *Nano Lett.* **2003**, *3*, 93–99. (d) Lee, D. C.; Mikulec, F. V.; Korgel, B. A. *J. Am. Chem. Soc.* **2004**, *126*, 4951–4957. (e) Ye, X.; Lin, Y.; Wang, C.; Wai, C. *Adv. Mater.* **2003**, *15*, 316–319. (f) Cott, D. J.; Petkov, N.; Morris, M. A.; Platschek, B.; Bein, T.; Holmes, J. D. *J. Am. Chem. Soc.* **2006**, *128*, 3920–3921.

(8) Li, Z.; Andzane, J.; Erts, D.; Tobin, J. M.; Wang, K.; Morris, M. A.; Attard, G.; Holmes, J. D. *Chem. Mater.* **2007**, *19*, 3043–3046.

(9) Huang, P.-H.; Lai, C.-H.; Huang, R. T. *J. Appl. Phys.* **2005**, *97*, 10C311–3.

(10) Tepper, T.; Ilievski, F.; Ross, C. A.; Zaman, T. R.; Ram, R. J.; Sung, S. Y.; Stadler, B. J. H. *J. Appl. Phys.* **2003**, *93*, 6948–6950.

(11) Cullity, B. D. Graham, C. D. *Introduction to Magnetic Materials*; IEEE Press/John Wiley & Sons, Inc.: Hoboken, NJ, 2009.

(12) (a) Lima, E.; Brandl, A. L.; Arelaro, A. D.; Goya, G. F. *J. Appl. Phys.* **2006**, *99*, 083908. (b) Goya, G. F.; Berquo, T. S.; Fonseca, F. C. *J. Appl. Phys.* **2003**, *94*, 3520.

(13) (a) Barreiro, A.; Hampel, S.; Rummeli, M. H.; Kramberger, C.; Gruneis, A.; Biedermann, K.; Leonhardt, A.; Gemming, T.; Buchner, B.; Bachtold, A.; Pichler, T. *J. Phys. Chem. B* **2006**, *110*, 20973–20977. (b) Smith, D. K.; Lee, D. C.; Korgel, B. A. *Chem. Mater.* **2006**, *18*, 3356–3364. (c) Pradhan, B. K.; Toba, T.; Kyotani, T.; Tomita, A. *Chem. Mater.* **1998**, *10*, 2510–2515.

(14) Koprinarov, N.; Konstantinova, M.; Ruskov, T.; Spirov, I.; Marinov, M.; Tsacheva, Ts. *Bulg. J. Phys.* **2007**, *34*, 17–32.

(15) Komada, T.; Sano, T.; Yoshida, T.; Tsuji, M.; Tamaura, Y. *Carbon* **1995**, *33*, 1443–1447.

JA105079Y